



Degradation of crystal violet by heterogeneous Fenton-like reaction using Fe/Clay catalyst with H₂O₂

M. Idrissi^{1,2}, Y. Miyah¹, Y. Benjelloun¹, M. Chaouch²

¹ QHSE Research Group, Laboratory of Catalysis, Materials and Environment, University of Sidi Mohammed Ben Abdellah, School of Technology, BP 2427 Fez – Morocco

² Laboratory LGME, Faculty of Sciences Dhar El Mahraz, University of Sidi Mohammed Ben Abdellah – Morocco

*Corresponding Author. E-mail: idrissi.meryem04@gmail.com

Abstract

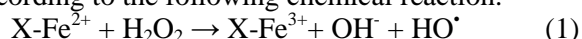
In this study, the heterogeneous Fenton-like degradation of Crystal violet (CV) in water was investigated over iron containing Clay prepared by impregnation. The sample was characterized for physical and chemical properties by XRD, SEM and FTIR measurements. The effects of various operating parameters like Metal loading in the catalyst variety, initial pH, hydrogen peroxide concentration and catalyst loading on the removal of dye, color and COD from an aqueous solution were studied at atmospheric pressure. The catalytic reaction obeyed first order kinetics. Although the Fe/Clay showed good performance for oxidation degradation of the dye, especially high catalytic activity with a wide pH range, the best catalytic results were achievable with Fe/Clay loading of 0.75 g/L with about 99% COD and 99% decolorization was achieved within 10 min treatment. It was also observed that catalytic behaviour could be reproduced in consecutive experiments with low iron leaching.

Keywords: Fenton-like reaction, Clay, impregnation, hydrogen peroxide, Decolorization, crystal violet.

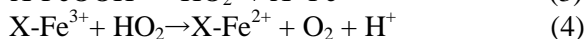
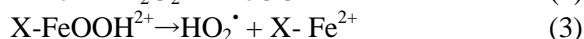
1. Introduction

Organic dyes are used in many industries such as textiles, pharmaceutical products, cosmetics, paint and varnishes, ink, plastics and optical data discs and computers[1]. The effluent from these industries, when it contains substantial amounts of such dyes, causes not only coloration of water, but also poses a threat to aquatic life [2]; furthermore, these solutions cause serious environmental problems when dyes containing industrial effluents are discharged into water bodies. On the other hand these dyes are toxic, carcinogenic and mutagenic[3]. Therefore, it is necessary to find an effective method for the wastewater treatment of reactive dyes. Majority of the conventional treatment methods comprise of adsorption [4], coagulation [5], filtration [6] and biological treatment[7]. In the last decade, attention has focused on the Advanced Oxidation Processes (AOP) that is based on the generation of highly reactive hydroxyl radicals. Among them, Fenton process has received a lot of attention and patronage because of rapid formation of HO[•] radicals with a high reaction yield and regeneration of the catalyst is possible. To overcome of heterogeneous Fenton process some attempts have been made to develop heterogeneous catalysts, prepared by loading iron (III) oxide onto a porous support such as clays, activated carbon and graphite using more or less simple techniques [8-10]. Clays have been reported to be good candidate as catalyst support because they are natural, abundant and cheap.

In the presence of H₂O₂, hydroxyl radicals (OH[•]) are produced by interaction of H₂O₂ with the iron (II) species present on the porous support according to the following chemical reaction:

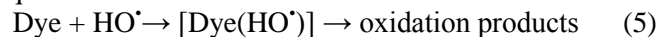


Where X presents the surface of the catalyst. Iron (III) can react with H₂O₂ in order to regenerate iron (II) supporting the Fenton process according to the following Equations 2–4:



the reduction–oxidation reactions between Fe(III)/Fe(II) take place in the presence of hydrogen peroxide which promote the formation of reactive components such as the hydroxyl ($\cdot\text{OH}$) and the hydroperoxyl ($\cdot\text{OOH}$) generated in Eq.3 are less reactive than the hydroxyl radicals.

The radicals generated by the decomposition of hydrogen peroxide can in turn react with the dyes resulting in the decolorization through Eqs. 5:



The main goal of this study was to investigate the applicability of iron impregnated oxide on Clay as heterogeneous Fenton catalyst for decolorization of Crystal violet. In order to improve the catalytic property of Fe/Clay. The effectiveness of this catalyst in decolorization of the dye and the effects of different parameters such as iron ions loading on supported catalyst, catalyst amount, initial concentrations of H_2O_2 and dye and initial pH of the dye solution would be assessed.

2. Experimental

2.1. Materials

The used clay originating in the area of Oulja, had the chemical composition 37,86% SiO_2 , 10,43% Al_2O_3 , 4,65% Fe_2O_3 , 0.06% MnO , 2,52% MgO , 18,72% CaO , 0.26% Na_2O , 2,34% K_2O .

Hydrogen peroxide (30%, w/w) and Ferric chloride hexahydrate ($\text{FeCl}_3 \cdot 6\text{H}_2\text{O}$) were purchased from Sigma–Aldrich. The dye of reactive Crystal Violet (99% pure) provided by the company Ciba Specialty Chemicals Inc. All the reagents used for this experiment were analytical grade and were used without further purification. The chemical structure of CV is shown in Figure 1.

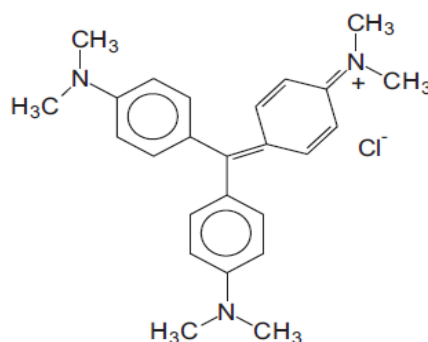


Figure 1: Chemical structure of crystal violet (CV).

2.2. Preparation of catalysts

The catalysts clay based, named xFe/Clay (where x is the iron weight percent in the calcined solid, $1 < x < 8$) were prepared by the wetness impregnation method. An amount of the support (Clay) was added to 50 mL of an aqueous solution of Ferric chloride (FeCl_3) containing the suitable amount of iron. The solution was left under stirred constantly kept at 120 rpm and in a Bain-marie at 100°C until all water was evaporated. After impregnation, the sample dried at 105°C in an oven for overnight, followed by calcination at 500°C for 4 h.

2.3. Characterization of catalyst

2.3.1. SEM-EDS analysis

Scanning electron microscope (SEM) was used to study the surface morphology of the Clay and Fe/Clay images were taken with a SEM-EDX,(Quanta 200 FEI) instrument equipped with probe EDAX for microanalysis of surfaces).

2.3.2. XRD analysis

The crystallographic structure of the catalyst and clay were established using powder X-ray diffraction (XRD) the Panalytical company using $\text{Cu K}\alpha$ ($\lambda = 1,54060 \text{ nm}$) radiation, functioning to 40 kV and 30 mA. The data were collected with $2\theta = 10^\circ - 80^\circ$.

2.3.3. FTIR analysis

Fourier transform infrared (FTIR) spectroscopy was conducted to study the surface chemistry of the Clay and Fe/Clay by identifying the functional groups presented on the samples using Model BRUKER (Vertex70).The spectra were measured from 7500 to 400 cm^{-1} .

2.3.4. XRF analysis

The clay characterized by X-ray fluorescence spectrometer (XRF), uses a sequential spectrometer AXIOS PANALYTICAL with a channel of measurement bases on only one goniometry covering the complete range of measurement of B to U.

2.4. Catalytic test

The amount of the dye present in the solution was analyzed by direct reading using a spectrophotometer (Jasco V530) with a spectrometric quartz cell (1 cm path length). The maximum absorbance of CV was measured at 588nm. All experiments were carried out in 200mL glass beaker containing 100 ml of an aqueous solution of 0.02g/L CV dye with an agitation for 60 min. Predetermined amounts of impregnated catalyst were then added to the beaker and the mixture was allowed to react for 15 min to reach equilibrium. After amount of H₂O₂ was added into the beaker this was recorded as the starting time of the reaction. The levy was carried out by filtered using a syringe filter of diameter 0,45μm to separate catalyst particles from the solution.

The reduction in the chemical oxygen demand (COD) of the dye solution was determined using a COD Reactor, HACH COMPANY after a reaction time of 1 h.

3. Results and discussion

3.1. SEM results

Figure 2 (A) and (B) shows the SEM images of Clay and impregnated Fe/Clay. It can be seen that surface morphology of the clay is different from the one impregnated. The incorporation of Fe into the Clay and calcination can be seen to have developed some voids in the Fe/Clay, and has also transformed into choppy layered structure characterized with increased pores[11], as a consequence of iron loading, this means that there was a rather uniform distribution of iron throughout the clay surface rather than an unusual deposit on it.

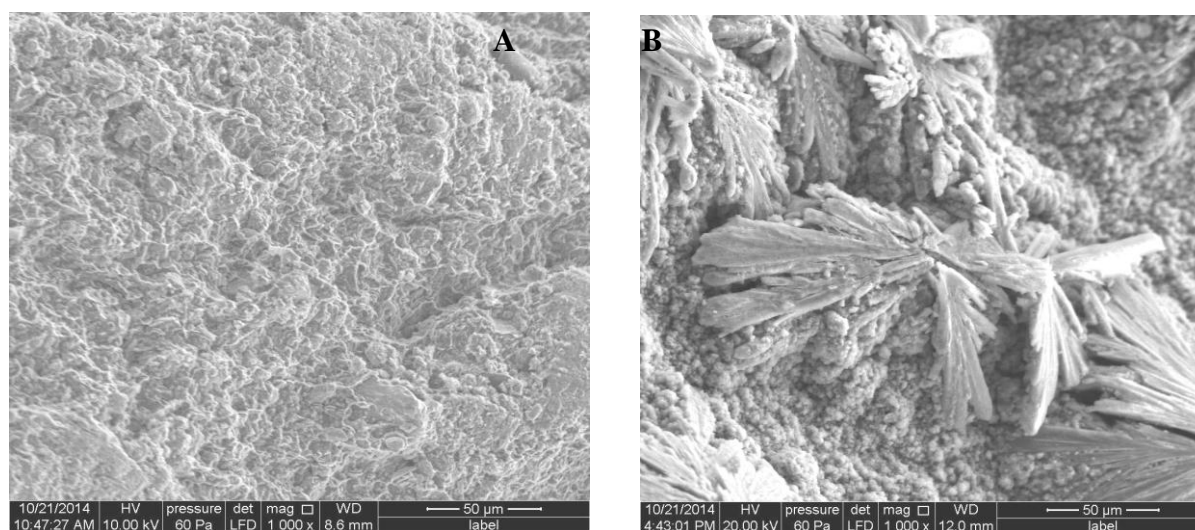


Figure 2: SEM images of (A) Clay and (B) 5% Fe/Clay.

3.2. XRD results

The X-ray diffraction spectra of the clay and catalyst were shown in Figure 3. For clay, the main mineral found is quartz with sharp and small diffraction peaks at 2θ of 20.94, 26.71, 36.62, 50.21, 60.02 and 64.73.

For diffractogram catalysts there is an appearance of new phases of oxides. In the Fe/clay catalyst the most intense peaks, ascribed to the characteristic reflections of crystalline Fe₂O₃, were observed at 24°, 32.8° and 35° [12]. Implying that of the metal oxide was fixed in the Clay by impregnation method.

3.3. FTIR results

The FTIR spectrums of the clay and Fe/Clay are shown in Figure 4. Molecules which are chemically bonded to the clay surfaces will change the FTIR spectra, whereas molecules adsorbed on the surface will have no effect on the FTIR vibrations of various groups present in clay [13]. The first two bands namely 3622 and 3392 cm⁻¹ which are identified in the O–H stretching region corresponding to Al–OH_{str} (octahedral structural hydroxyl groups) [14, 15]. The peaks at 1634 and 1633 cm⁻¹ indicated the presence of hydroxyls due to superficially

adsorbed and interlayer water. The bands at 1456 and 1423 cm^{-1} is due to the bending vibration mode of physisorbed water on the surface of free silica [16]. The band centered at 1001 cm^{-1} may be typically assigned to the Si–O stretching. The band at 981.73 cm^{-1} is attributed to the deformation vibrations of hydroxyl groups; Al–O–H sitting on the alumina faces [17]. Typical bands of the silicate framework contributions were confirmed: at 1001 cm^{-1} due to in-plane band stretching of Si–O bonds; at 695 and 516 cm^{-1} , corresponding to Si–O–Si and Al–O–Si vibrations [18].

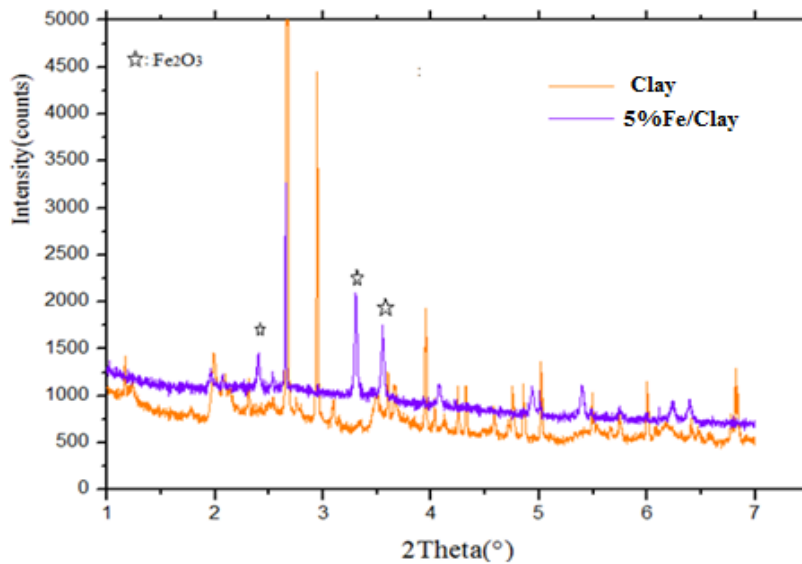


Figure 3: XRD Patterns of Clay and Fe/Clay.

Spectra for the modified clay, the bands intensity increased slightly due to hydration water effects, after being impregnated.

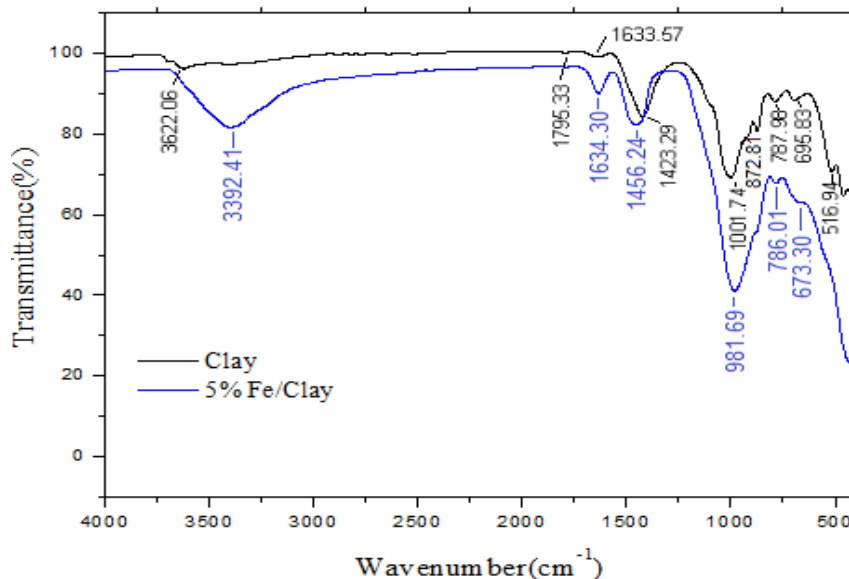


Figure 4: FTIR spectra of Clay and 5% Fe/Clay.

3.4. Factors affecting removal efficiency

3.4.1. Decolorization kinetics of the Fenton-like oxidation of CV

One of the primary aims of this investigation was to gain an insight into the process of the CV decolorization by Fe/Clay. Comparative experiments were conducted in this research under different reaction conditions: H_2O_2 only, catalyst only, and catalyst and H_2O_2 . Figure 5 shows the results obtained.

The results show that H₂O₂ alone is not an effective process for the treatment of CV we have observed a Low and negligible decolorization rate this behavior might be due to the limited oxidation ability of H₂O₂ compared to hydroxyl radical. Whereas When Fe/Clay was used, less than 30% decolorization of CV was achieved because of adsorption capability of the catalyst. However, with simultaneous presence of catalyst and H₂O₂, decolorization efficiency was 99 % within 10 min. According to these results we can say that the presence of Fe/Clay greatly improved the oxidative ability of H₂O₂ by the catalytic reactions that occurred between coated iron oxides and H₂O₂ for the removal of CV.

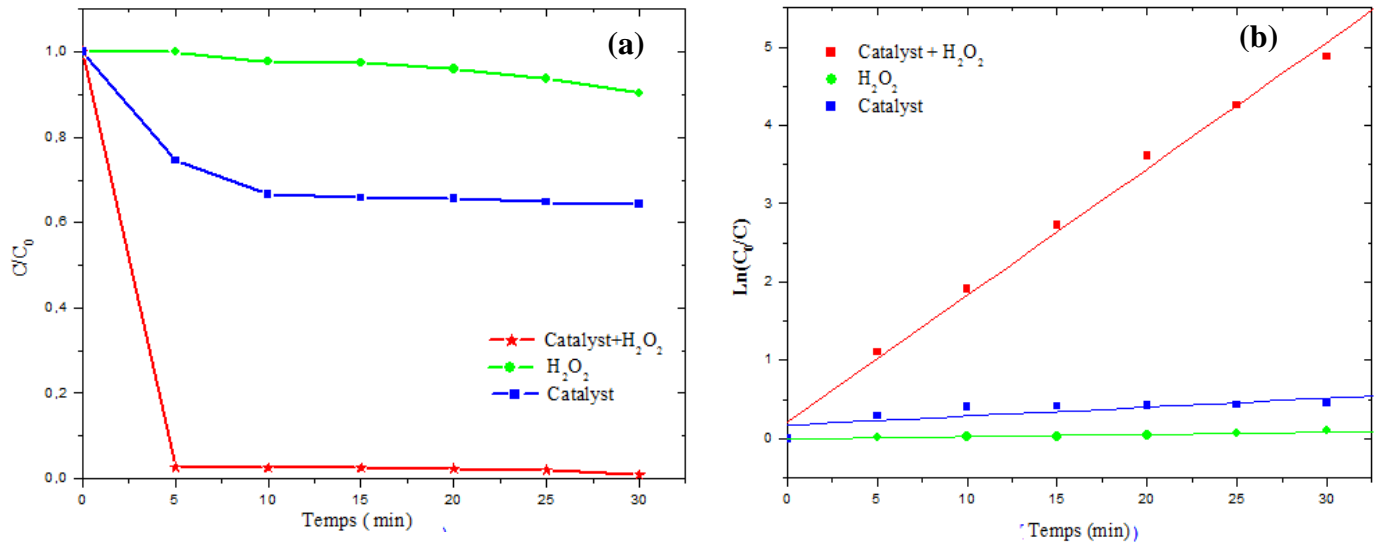


Figure 5: (a) Decoloration of CV at different experimental conditions; (b) CV degradation kinetics during the Fenton processes. ([CV]₀ = 0.02g/L, catalyst dosage = 0.75 g/L with 5% Fe/Clay, pH of solution, 2ml of H₂O₂, initial concentration of hydrogen peroxide, [H₂O₂]₀ = 0.1M).

The kinetic measurements were carried out under pseudo-first order conditions. *k*, was determined from graphical fit (Figure 5) to the following equation:

$$\ln(C_0/C_t) = A + Kt \quad (6)$$

Where *C_t* is the concentration of dye at time = *t*, *C₀* the initial concentration of dye, **K** the decolorization rate constant (min⁻¹) and **A** an experimental constant. The *k* (Table 1) was determined from the slope of the plot $-\ln(C_t/C_0)$ versus time (*t*). The straight lines in the plot indicate that the decolorization rate is pseudo-first order with respect to *C₀*.

Table 1: Kinetic constants of the first order plot

	Fe/Clay + H₂O₂	H₂O₂	Fe/Clay
K(min⁻¹)	0.161	0.003	0.0115
R	0.99	0.94	0.78

3.4.2. Effect of catalyst loading

Figure 6. shows the effect of catalyst iron loading on the decolorization of CV. The results indicated that the decolorization of CV is dependent on the iron ions concentration (2.5% to 7.5%) at fixed initial concentration of hydrogen peroxide and CV. As the catalyst loading increased to 5%Fe the performance of decolorization was almost same with loading 2.5%Fe catalyst. However, as the catalyst loading increased to 7.5%Fe a decreased performance of decolorization could be observed. The better decolorization reached 99% by 5% Fe/Clay when reaction time was 10 min. This phenomenon may be caused by increase of the amount of ferric ions involved in the process resulted in an increase in the number of ·OH radical significantly[19].

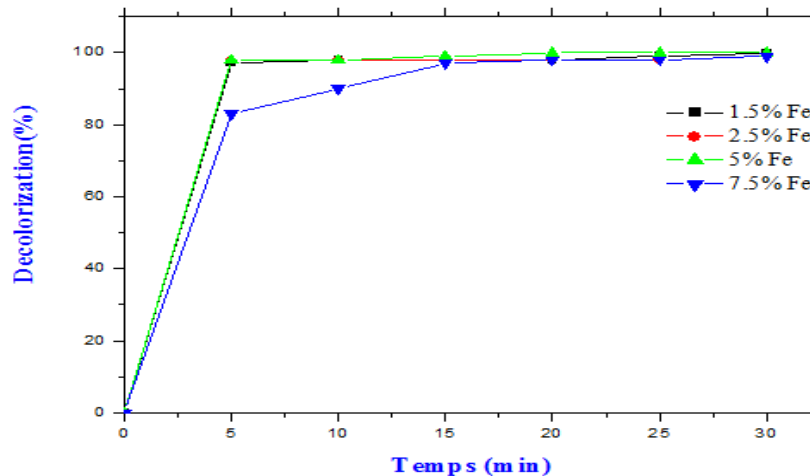


Figure 6: Effect of iron loading on Clay on the decolorization of CV. Reaction conditions: initial concentration of CV, $[CV]_0 = 0.02 \text{ g L}^{-1}$, 2ml of H_2O_2 , initial concentration of hydrogen peroxide, $[\text{H}_2\text{O}_2]_0 = 0.1 \text{ M}$, pH of solution, dosage of catalyst = $0,075 \text{ g L}^{-1}$.

3.4.3. Influence of the hydrogen peroxide concentration on the degradation of dye

The influence of hydrogen peroxide concentration on the oxidation of the dye by Fe/clay as catalyst was examined by varying initial concentration of H_2O_2 from 0.05M to 0.2M while maintaining constant all the other operating parameters, the results is presented in Figure 7. The decolorization efficiency of CV increased when hydrogen peroxide concentration increased from 0.05 to 0.1 M. However, further increase in concentration of H_2O_2 (0.2M) caused a negative effect for the color removal.

The reaction went more slowly when the concentration was lower (0.05 M) or higher (0.2 M). At low concentration, H_2O_2 cannot generate enough radical $\cdot\text{OH}$ and the oxidation rate is logically slow. The increase of the oxidant concentration from 0.05 to 0.1 M led to an increase in the reaction rate, as expected, because more radicals will be formed. Nevertheless, for a very high H_2O_2 concentration (0.2 M), the performance decreased. At higher H_2O_2 concentrations, once radicals have been generated, they are exhausted through scavenging reaction mechanisms by hydrogen peroxide itself to form hydroperoxyl radicals (Eq. 7) with a lower oxidizing power [11, 20, 21]; the latter can also scavenge hydroxyl radicals according to Eq.8[20]:

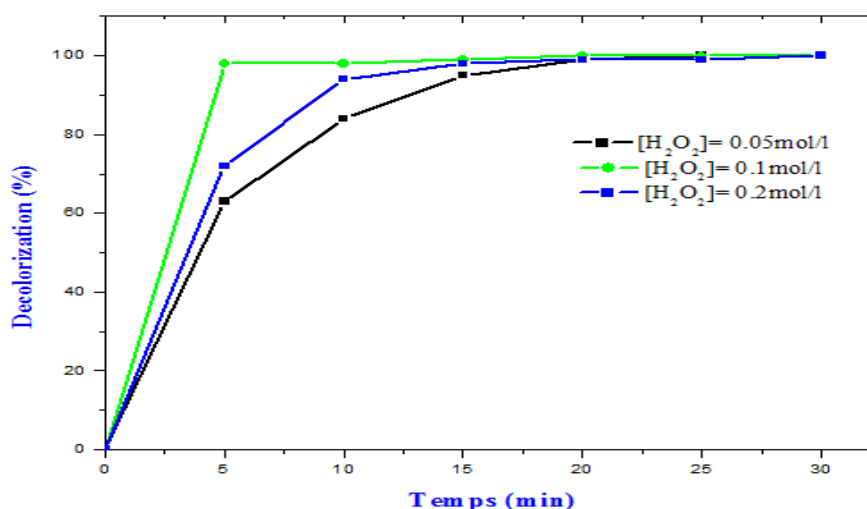
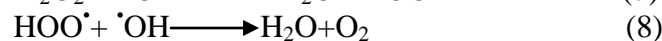


Figure 7: Effect of initial concentration of hydrogen peroxide on the decolorization of CV. Reaction conditions: initial concentration of CV, $[CV]_0 = 0.02 \text{ g/L}$, catalyst dosage = 0.75 g/L with 5% Fe/Clay, pH of solution.

3.4.4. Effect of catalyst dosage

The influence of the catalyst amount was investigated on decolorization efficiency against time using catalyst dosage of 25 mg at 100 mg for 0.02g/l dye (CV) solution. The results are illustrated in Figure 8. The result followed a well-known trend in the Fenton process, where the decolorization rate increases with the increase in catalyst concentration until reaching a maximum, because more catalyst active sites were available for hydroxylation of the HO^\bullet , and then the decolorization rate slightly decreased upon further addition of the catalyst [22-24] caused by the inhibition effect of iron species because the scavenging of hydroxyl radicals or other radicals occurs when presenting excessive metal species, which can be expressed by the following equations [25-27].



Thus, it could be concluded that the optimum catalyst is 0.75 mg/L.

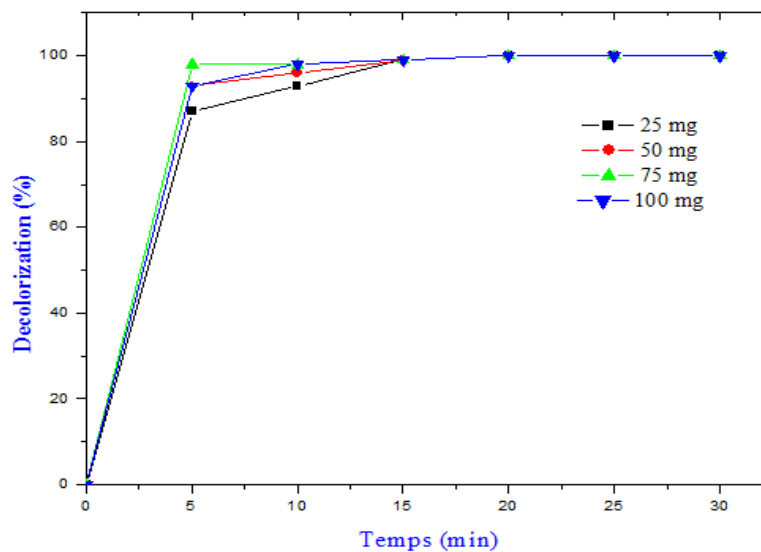


Figure 8: Effect of dosage of catalyst on the decolorization of CV. Reaction condition: initial concentration of CV, $[\text{CV}]_0 = 0.02 \text{ g L}^{-1}$, 2ml of H_2O_2 , initial concentration of hydrogen peroxide, $[\text{H}_2\text{O}_2]_0 = 0.1 \text{ M}$, pH of solution, 5% Fe/Clay.

3.4.5. Effect of pH

The effect of initial pH value on the decolorization of CV was studied in the pH range of 3.0–9.0 and the result is as shown in Figure 9.

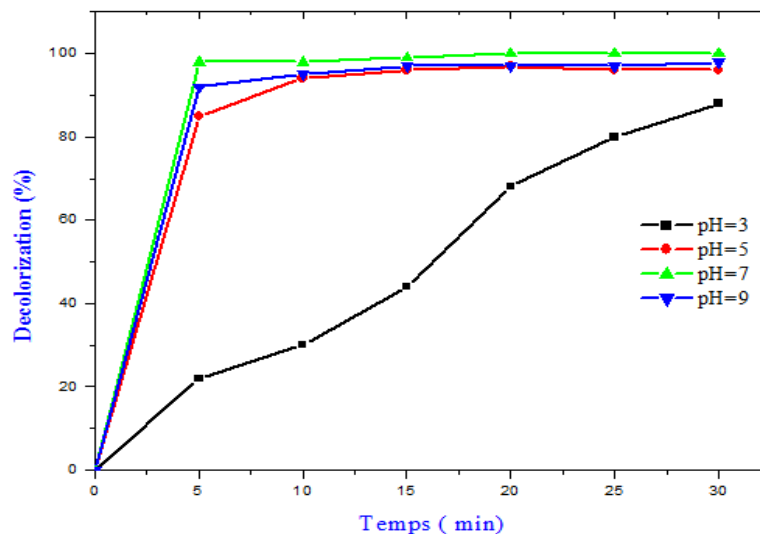


Figure 9: Effect of pH on the decolorization of CV. Reaction conditions: initial concentration of CV, $[\text{CV}]_0 = 0.02 \text{ g L}^{-1}$, 2ml of H_2O_2 , initial concentration of hydrogen peroxide, $[\text{H}_2\text{O}_2]_0 = 0.1 \text{ M}$, dosage of catalyst = 0.75 g L^{-1} with 5% Fe/Clay.

The results showed that the optimum solution pH for decolorization of CV was achieved at pH 7 with 100% decolorization efficiency within 5 min reaction time, the decolorization reaction slightly decreased as increasing pH from 7 to 9. However, at pH 3, only 22 % decolorization efficiency was gained at same reaction time.

The surface charge of catalyst was also influenced by pH value. The point of zero charge (pZc) of catalyst was about 8.02. When pH was near 8.02, catalyst was in the form negatively charged and crystal violet was in the form of positively charged, and had strong electrostatic attraction with Fe on the surface of catalyst. Therefore, crystal violet was easier to contact with active sites, and then was effectively decolorized.

When the solution pH was up inferior to 8, Crystal violet and the catalyst were positively charged. So they were mutually exclusive. Crystal violet could not contact with active sites, thus the decolorization efficiency decreased significantly.

3.4.6. Stability of the catalyst

The reuse and leaching tests were performed in order to evaluate the catalytic activity of Fe/Clay during successive experiments and thus to observe the possibility of catalyst reuse. Samples were analyzed to determine the concentration of dissolved iron ions. The amount of leached iron was 0.026 mg/L after 60 min. the runs were carried out using an 100 ml of 0.02 g/L CV aqueous solution with an addition of 0.1 M H₂O₂ at a pH of solution. After each run, the catalyst was removed by filtration and then washed with distilled water for several times and dried at 100°C for 12 h. Then the catalyst was reused with a fresh Crystal violet solution. The results are summarized in Figure 10. Show that the activity decreased gradually during successive runs. However, the removal rate was rather comparable for all the runs at longer reaction times. It could be seen that the catalyst remain 86% CV removal efficiency after four consecutive runs under the same reaction condition.

The decrease of catalytic activity can be attributed to two reasons: first, the poisoning of the active catalytic sites due to the adsorbed organic species. Second, the iron leaching may be another important factor that could cause the loss of activity of the catalyst [28-30].

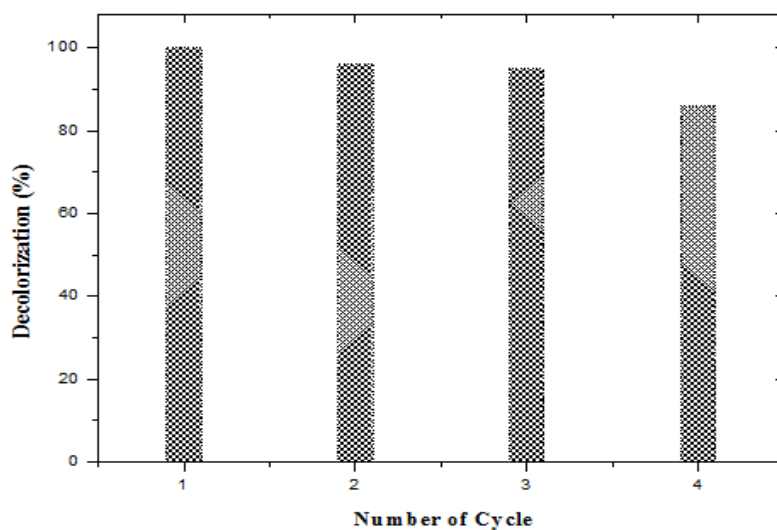


Figure 10: Reusability and stability of catalyst

Conclusion

This paper described the characterization and catalytic performance of the iron containing Clay prepared by impregnation over the heterogeneous Fenton-like degradation of dye Crystal violet which is representative of water contaminant. This catalyst showed good performance for oxidation degradation of dye (CV), especially high catalytic activity with a wide pH range. Physico-chemical characterization of the catalyst evidenced successful immobilization of the Fe on the clay. A complete color removal could be achieved with the catalyst at a pH of 7 in an H₂O₂ concentration of 0.1M, 5% of iron ions loading, 0.75g/L of catalyst dosage for 20 mg/L initial CV concentration.

Under these conditions, 99% decolorization efficiency of CV in aqueous solution was achieved within 10 min of reaction time. The advantages of this process include recyclable Fe/Clay catalyst with a reasonable small iron leaching which makes possible for the catalysts to have long term stability and no iron sludge formation.

It can be concluded that this study may provide useful information for the use of low cost materials, based clay iron containing as catalysts in heterogeneous Fenton process catalysts for the degradation of CV aqueous solutions.

References

1. Miyah Y., Idrissi M., Zerrouq F., *Journal of Materials and Environmental Science* 6 (2015) 699-712.
2. Kondru A.K., Kumar P., Chand S., *Journal of Hazardous Materials* 166 (2009) 342-347.
3. Zhu M., Meng D., Wang C., Di J., Diao G., *Chinese Journal of Catalysis* 34 (2013) 2125-2129.
4. El Gaidoumi A., Chaouni B.A., Lahrichi A., Kherbeche A., *JMES* 6 (8) (2015) 2247-2259.
5. Riera-Torres M., Gutiérrez-Bouzán C., Crespi M., *Desalination* 252 (2010) 53-59.
6. Nataraj S.K., Hosamani K.M., Aminabhavi T.M., *Desalination* 249 (2009) 12-17.
8. Daud N.K., Hameed B.H., *Journal of Hazardous Materials* 176 (2010) 938-944.
9. Idrissi M., Lamonier J.-F., Chlala D., Giraudon J.-M., Chaouch M., Miyah Y., Zerrouq F., *J. Mater. Environ. Sci.* 5 (2014) 2303-2308.
10. Idrissi M., Miyah Y., Chaouch M., El Ouali Lalami A., Lairini S., Nenov V., Zerrouq F., *J. Mater. Environ. Sci.* 5 (2014) 2309-2313.
11. Azmi N.H.M., Ayodele O.B., Vadivelu V.M., Asif M., Hameed B.H., *Journal of the Taiwan Institute of Chemical Engineers* 45 (2014) 1459-1467.
12. Ayodele O.B., Hameed B.H., *Journal of Industrial and Engineering Chemistry* 19 (2013) 966-974.
13. Monash P., Niwas R., Pugazhenth G., *Clean Techn Environ Policy* 13 (2011) 141-151.
14. Madejová J., *Vibrational Spectroscopy* 31 (2003) 1-10.
15. Hassan H., Hameed B.H., *Chemical Engineering Journal* 171 (2011) 912-918.
16. Zuo S., Zhou R., Qi C., *Journal of Rare Earths* 29 (2011) 52-57.
17. Konan K.L., Peyratout C., Smith A., Bonnet J.P., Rossignol S., Oyetola S., *Journal of Colloid and Interface Science* 339 (2009) 103-109.
18. Nogueira F.G.E., Lopes J.H., Silva A.C., Lago R.M., Fabris J.D., Oliveira L.C.A., *Applied Clay Science* 51 (2011) 385-389.
19. Kumar P., Agnihotri R., Mondal M.K., *Journal of Environmental Chemical Eng.* 1 (2013) 440-447.
20. Fathy N.A., El-Shafey S.E., El-Shafey O.I., Mohamed W.S., *Journal of Environmental Chemical Engineering* 1 (2013) 858-864.
21. Zhan Y., Zhou X., Fu B., Chen Y., *Journal of Hazardous Materials* 187 (2011) 348-354.
22. Liao Q., Sun J., Gao L., *Colloids and Surfaces A: Physicochemical and Engineering Aspects* 345 (2009) 95-100.
23. Kuang Y., Wang Q., Chen Z., Naidu R., *Journal of Colloid and Interface Science* 410 (2013) 67-73.
24. Chen Y., Li N., Zhang Y., Zhang L., *Journal of Colloid and Interface Science* 422 (2014) 9-15.
25. Bokare A.D., Choi W., *Journal of Hazardous Materials* 275 (2014) 121-135.
26. Ramirez J.H., Maldonado-Hódar F.J., Pérez-Cadenas A.F., Moreno-Castilla C., Costa C.A., Madeira L.M., *Applied Catalysis B: Environmental* 75 (2007) 312-323.
27. Romero A., Santos A., Vicente F., *Journal of Hazardous Materials* 162 (2009) 785-790.
28. Cao G., Sheng M., Niu W., Fei Y.-l., Li D., *Journal of Hazardous Materials* 172 (2009) 1446-1449.
29. He W., Ma Q., Wang J., Yu J., Bao W., Ma H., Amrane A., *Applied Clay Science* 99 (2014) 178-186.
30. Yang B., Tian Z., Zhang L., Guo Y., Yan S., *Journal of Water Process Eng.* 5 (2015) 101-111.

(2016) ; <http://www.jmaterenvirosci.com>